Colloid-Polymer Mixtures at Triple Coexistence: Kinetic Maps from Free-Energy Landscapes

W. C. K. Poon, F. Renth, R. M. L. Evans, D. J. Fairhurst, M. E. Cates, and P. N. Pusey
Department of Physics and Astronomy, The University of Edinburgh, Mayfield Road, Edinburgh EH9 3JZ, Scotland
(Received 6 April 1999)

We have studied the kinetics of phase separation in a colloid-polymer mixture. The evolution of initially homogeneous samples as they separate into coexisting colloidal gas, liquid, and crystal phases was investigated by time-lapse video recording. Distinct kinetic regimes were found, the existence and character of which are interpreted in terms of the "free energy landscape" of the system.

PACS numbers: 82.70.Dd

Understanding the kinetics of phase separation is both a challenge to fundamental physics and of considerable technological importance. Progress is slow partly because of the intrinsic difficulty of the theory [1]. There are also few experimental paradigms due to the scarcity of model systems that allow access to the full range of length and time scales—from early stages to final equilibrium.

In this Letter, we present experiments on phase transition kinetics in a model colloid-polymer mixture [2]. Initially homogenized samples evolve over hours or days towards final states in which macroscopic regions of colloidal gas, liquid, and crystal phases coexist in thermodynamic equilibrium. By varying the sample composition, we identify several distinct kinetic regimes in which the three phases emerge along distinctive pathways. We explain the occurrence and location of these regimes by considering the underlying (mean-field) free energy of the material. Apart from advancing our understanding of a system central to recent research in colloid physics [3], our work has considerable generic interest. First, most fundamental studies of phase transitions kinetics to date [1] have concentrated on the emergence of *two* phases. Below we find several novel features concerning the evolution towards *three*-phase coexistence. Second, while the rest of the paper is couched in terms of "gas," "liquid," and "crystal" phases in a colloid-polymer mixture, our approach should be applicable to *any* condensed system separating into three (or more) phases with different structures—there is a generic link [4] between phase pathways and the free energy "landscape."

The experimental system consists of hard-sphere-like sterically stabilized polymethylmethacrylate particles suspended in cis-decalin, with radius $R = 240 \pm 5$ nm and polydispersity $\lesssim 5\%$. A nonadsorbing polymer, linear polystyrene (PS), of molecular weight $M_w = 7.3 \times 10^6$ and radius of gyration $r_g = 88$ nm is added. Polymer segments are depleted from a layer of thickness $\sim r_g$ around each particle. The overlap of the "depletion layers" of two particles creates additional free volume for the polymer, lowers the free energy, and causes an interparticle "depletion" attraction,

$$U_{\mathrm{dep}}(r) \simeq -\Pi_p V_{\mathrm{ov}}\,, \tag{1}$$

where Π_p is the osmotic pressure of the polymer, and V_{ov} is the overlap volume of neighboring depletion layers. PS is nearly ideal in cis-decalin at room temperature, so that $\Pi_p \approx n_p^* k_B T$, where n_p^* is the number density of polymer chains *in the free volume.* For ideal polymers, n_p^* is related to the polymer chemical potential μ_p (and its thermal wavelength Λ_p) by [5]

$$n_p^* = \Lambda_p^{-3} e^{\mu_p/k_B T}. \tag{2}$$

The topology of the phase diagram of a colloid-polymer mixture depends on the size ratio, $\xi = r_g/R$ [5]. The calculated phase diagram for $\xi \sim 0.4$ is shown schematically in Fig. 1 in the (ϕ, μ_p) representation (ϕ is the colloid volume fraction). Triple coexistence of colloidal gas, liquid, and crystal phases occurs along a *line* at a particular polymer chemical potential, μ_p^{tr}. Experimentally, the

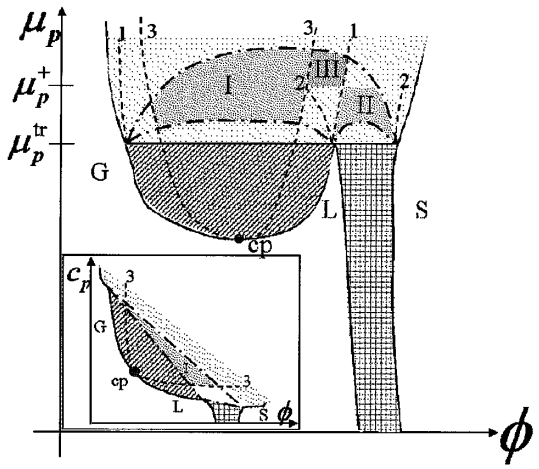

FIG. 1. Theoretical phase diagram [5] in the (ϕ, μ_p) plane. gas(G)-liquid(L), liquid(L)-solid(S), and gas-solid coexistence occur in hatched, doubly hatched, and dotted areas, respectively; cp: critical point. Triple coexistence occurs at μ_p^{tr}. Dotted curves: G-L (1-1) and L-S (2-2) binodals, and G-L spinodal (3-3); these are *metastable* for $\mu_p > \mu_p^{\mathrm{tr}}$. The L-S binodal terminates at $\mu_p^{\dagger}$, where it meets the G-L spinodal. The area enclosed by the dot-dashed curves maps onto the triple-coexistence triangle in the (ϕ, c_p) representation (see inset). Within the shaded regions labeled I, II, and III we predict corresponding kinetic pathways discussed in the text. Inset: (ϕ, c_p) representation of the same system; lines and shadings mean the same as in the main diagram (regions II and III are too small to be labeled in this representation).

control variable is the polymer number density in the *total* volume, n_p (or, equivalently, the total polymer *mass* concentration c_p). Since c_p is different for the three phases at triple coexistence, the three points along the triple *line* now becomes the vertices of a *triangle* in the (ϕ, c_p) plane (inset, Fig. 1) [5]. The equilibrium state of any sample within the triangle is coexistence of colloidal gas, liquid, and crystal phases with compositions given by the three corners of the triangle. Crucially, *homogeneous* samples with compositions within the triple triangle are mapped nonlinearly onto a "bat"-shaped domain in the (ϕ, μ_p) plane (Fig. 1). Thus, a homogenized sample, within the triple triangle, has $\mu_p > \mu_p^{\rm tr}$; as phase separation proceeds, μ_p drops continuously, until $\mu_p = \mu_p^{\rm tr}$ when three-phase separation is complete. The experimental phase diagram for our system ($\xi = 0.37$) is shown in Fig. 2.

We prepared a series of samples in 1 cm × 4 cm × 2 mm optical cells with compositions within the triple coexistence triangle. These were homogenized by prolonged tumbling, and then left undisturbed for observation using time-lapse video recording in transmitted, collimated white light [6]. Gas, liquid, and crystalline phases appear in the video image as regions of different transmission. Monitoring by eye was also carried out under reflected light to identify iridescent crystalline regions; these are not visible in the transmission images shown below, but assisted phase identification. Otherwise, phases were distinguished by their different transmissions (gas appeared brightest), aided by comparison with the final state, where their identification is unambiguous.

In different areas of the triple triangle, various distinct kinetic routes to final three-phase coexistence were observed. We present three examples (for more details of these and others, see [6]). Regime 1 occupies a large central section of the triangle. Here, rapid demixing into gas and liquid phases was observed. The rapidity of the demixing, and the observation of a brightening and collapsing small-angle ring of intensity in the scattering of laser light from these samples, suggests the spinodal decomposition mechanism. After the formation of a sharp gas-liquid boundary, iridescent crystallites appeared in the liquid part of the sample and sank downwards. Figure 3 shows behavior typical of regime 1 (sample 1 of Fig. 2).

All other kinetic regimes occupy smaller areas in the triple triangle [6]. Regime 2 is found near the liquid-crystal edge; sample 2 (Fig. 2) is typical of it. This sample nucleated crystallites after a few hours, giving an iridescent lower phase and an amorphous upper phase of similar transmission to the initial homogeneous sample: crystal and liquid. Subsequently, a very dilute amorphous phase, gas, appeared at the top. At our experimental resolutions, we could not tell whether the gas had nucleated from within the liquid or the crystal phase, or from both.

Regime 3 is found just below the gas-crystal edge, and to the right of the liquid corner of the triple triangle. The resulting evolution (sample 3, Fig. 2) is shown in Fig. 4. The initially homogeneous sample gave rise rapidly to a thin layer of dilute gas at the top. Simultaneous with this, iridescent crystallites were seen (by eye) in the main body of the sample. As these sank and gathered at the bottom of the sample cell to form a polycrystalline region, the uppermost (gas) region grew in size, and a middle layer of liquid phase formed. Both gas-liquid and liquid-crystal interfaces appeared sharp at this stage. Subsequently, the gas-liquid interface seemed to become smeared out and "reform" at a lower position; at the same time, the liquid-crystal interface continuously moved downwards by approximately the same amount as the displacement of the gas-liquid interface. The observed "compression" of the crystal region is not due to the compaction of crystallites: there was virtually no change in the lattice parameter as the phase volume shrank [6].

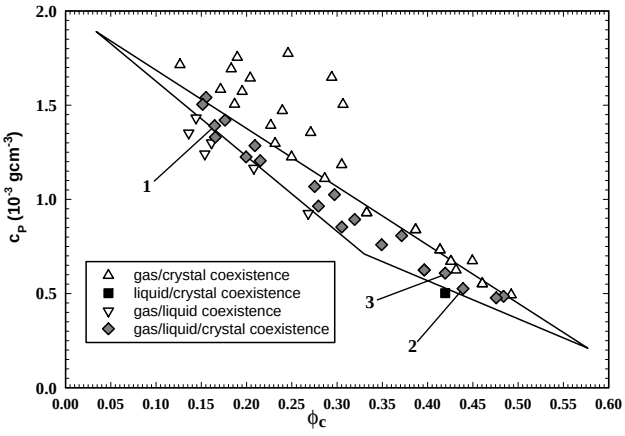

FIG. 2. Experimental phase diagram for our colloid-polymer mixture (see text). Horizontal and vertical axes are the colloid volume fraction ϕ and the polymer concentration c_p. The three-phase region encloses all three-phase samples and no two-phase samples, and must be a triangle. Hence, we can estimate it accurately, as shown. Samples labeled 1,2,3 lie in kinematic regimes 1,2,3.

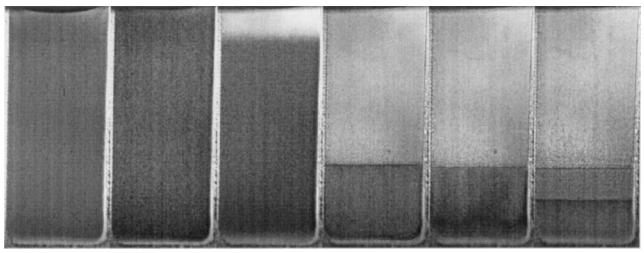

FIG. 3. The evolution of sample 1, after homogenization at time $t = 0$. From left to right: $t = 0$, homogeneous sample; $t = 2$ h 15 min, sample darkens, presumably due to the presence of droplets of the liquid phase throughout the sample; $t = 5$ h 30 min, darker, liquid phase begins to settle, giving rise to a diffuse gas-liquid interface; $t = 16$ h 15 min, well developed, metastable gas-liquid coexistence; $t = 21$ h 15 min, crystallites nucleate in the liquid phase—these show up as darker patches in the lower, liquid phase (and are iridescent to the naked eye); $t = 42$ h 15 min, final gas-liquid-crystal coexistence.

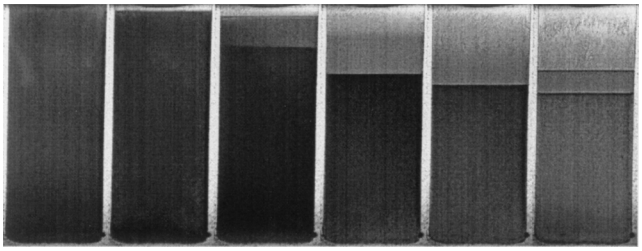

FIG. 4. Evolution of sample 3 of Fig. 2, homogenized at $t = 0$. From left to right: $t = 0$, homogeneous sample; $t = 4$ h 15 min, dilute gas appears on top and crystallites (iridescent to the naked eye) are seen throughout the denser part; $t = 6$ h 15 min, crystallites have settled, sharp gas-liquid and liquid-crystal interfaces are seen, with the crystal phase presumably made up of crystallites coated by thin layers of gas; $t = 12$ h 15 min, gas-liquid interface becomes fuzzy and crystal phase is shrinking in volume; $t = 20$ h 15 min, gas-liquid interface very smeared out, and bottom crystal phase continues to shrink in volume; $t = 60$ h 15 min, final gas-liquid-crystal coexistence. Compare the third and final images: The liquid phase volume is almost constant, and the decrease in crystal phase volume is roughly the same as the increase in gas phase volume.

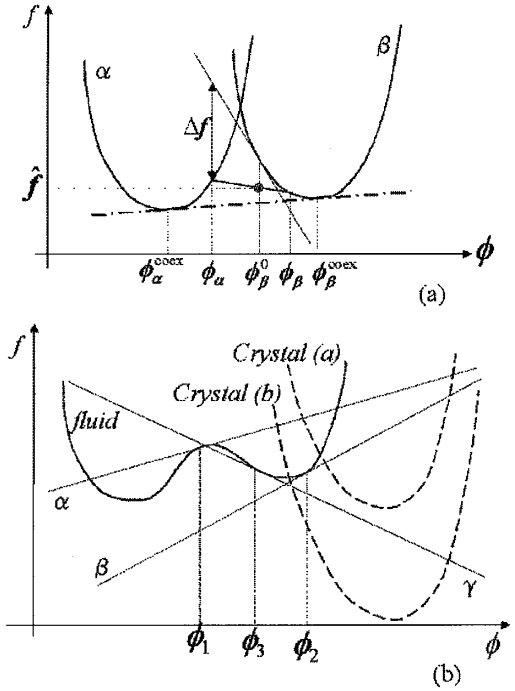

FIG. 5. Schematic free-energy landscapes $f(\phi)$. (a) α and β branches. A homogeneous sample of phase β at density ϕ_β^0 separating into phases at densities ϕ_α and ϕ_β lowers the free-energy density to $\hat{f}$. The maximal lowering of free energy occurs when the new phases have compositions $\phi_\alpha^{\rm coex}$ and $\phi_\beta^{\rm coex}$ given by the points of common tangency. The thermodynamic "driving force" available to create an *infinitesimal* amount of phase α at density ϕ_α out of a homogeneous phase of β at density ϕ_β^0 is given by Δf. (b) (i) Fluid and crystal (a) branches: our landscape for $\mu_p < \mu_p^\dagger$. A homogeneous sample with density ϕ_1 shows regime 1 behavior—the tangent α lies above the gas, liquid, and solid minima. A sample at ϕ_2 shows regime 2 behavior—the tangent β is above the solid minimum but below the gas minimum, so that, initially, only crystal nuclei can be formed. (ii) Fluid and crystal (b) branches: landscape for $\mu_p > \mu_p^\dagger$: a sample at density ϕ_3 will show regime 3 behavior—the tangent γ is above the solid and gas minima, but no liquid-solid common tangent can be constructed: any nucleated crystallite must coexist with a "coating" of gas.

We now link our observation of distinctive kinetic pathways, in different areas of the three-phase triangle, to the geometry of the underlying free energy landscape of the colloid-polymer mixture. This landscape, for a given μ_p, is a plot of the free-energy density (in the semigrand ensemble [5]) as a function of volume fraction, $f(\phi)$. Our approach extends a classic argument due to Cahn [4]. Consider first an $f(\phi)$ with two convex branches $f_\alpha(\phi)$ and $f_\beta(\phi)$, belonging to phases α and β [Fig. 5(a)]. A homogeneous phase of β at volume fraction ϕ_β^0, if it separates into two phases with densities ϕ_α and ϕ_β (conserving volume and mass), lowers its free-energy density to $\hat{f}$ [Fig. 5(a)]. The volume fractions of the two coexisting phases that *minimize* this free energy are given by the points of common tangency to $f_\alpha(\phi_\alpha^{\rm coex})$ and $f_\beta(\phi_\beta^{\rm coex})$. Now consider the change Δf in free energy, on formation of an infinitesimal amount of phase α at volume fraction ϕ_α out of a bulk phase of β at volume fraction ϕ_β^0. Δf is given by the vertical distance between the tangent to $f_\beta(0)$ at $\phi = \phi_\beta^0$, and the point $f_\alpha(\phi_\alpha)$ on the other free-energy branch—see Fig. 5(a) [4].

In colloid-polymer mixtures, $f(\phi)$ has a fluid branch (gas/liquid) with one or two minima, and one further minimum in a solid (crystal) branch [5,7]. The resulting landscape is controlled by the depth of the depletion potential, and, hence, the polymer chemical potential, [Eqs. (1) and (2)]. A sample which has macrophase separated into coexisting gas, liquid, and crystal regions has $\mu_p = \mu_p^{\rm tr}$ (Fig. 1); in its $f(\phi)$ plot, the three minima lie on a single common tangent. However, this sample homogenized will have $\mu_p > \mu_p^{\rm tr}$, and the liquid minimum lies *above* the common tangent between the gas and solid minima [see Fig. 5(b)].

As described below, the permitted kinetic routes are determined (for given initial ϕ) by the relative positions of these minima, and, hence, depend on the location of the sample within the bat-shaped domain in Fig. 1. This domain is divided into distinct regions by the various *metastable* spinodal and binodal curves, and by the line $\mu_p = \mu_p^\dagger$ (Fig. 1). Samples from each region should approach the final state of coexisting gas, liquid, and crystal phases by a different kinetic route.

Consider first samples with $\mu_p < \mu_p^\dagger$; the appropriate $f(\phi)$ is given by the "fluid" and "crystal (a)" branches in Fig. 5(b). A sample with colloid volume fraction ϕ_1 comes from region I in Fig. 1. The tangent α lies above all three minima, which means that, in principle, a homogeneous sample with this composition could form gas, liquid, or crystals. In practice, since ϕ_1 is within the spinodal region of the fluid branch ($\partial^2 f/\partial\phi^2 < 0$), we expect the gas-liquid separation to be fast and to occur

first, to be followed by the nucleation of crystals. This pathway is expected throughout the metastable spinodal region I (including $\mu_p > \mu_p^\dagger$). This behavior was found in "regime I" on the experimental three-phase triangle [8]. Staying with the fluid and crystal (a) branches in Fig. 5(b), a sample with volume fraction ϕ_2 comes from region II in Fig. 1. The tangent β lies above the crystal minimum, but below the gas minimum. We therefore expect such a sample to nucleate *crystals* out of the parent liquid phase first. This will rotate the tangent clockwise, eventually permitting the nucleation of gas. This is the experimentally observed "regime 2" behavior.

Now consider the fluid and "crystal (b)" branches in Fig. 5(b). A sample with volume fraction ϕ_3 comes from region III in Fig. 1. The tangent γ lies above both the gas and the crystal minima. Thus, a homogeneous sample of this composition may, initially, nucleate gas droplets and crystallites. This we observed for our experimental samples in "regime 3." However, since $\mu_p > \mu_p^\dagger$ here, no common tangent exists between the solid and the liquid minima [Fig. 5(b)] so that crystals *cannot coexist* with liquid. But common tangents between gas-liquid and gas-crystal minima can still be constructed, so that local equilibria between these pairs of phases are permitted. To satisfy these constraints, any crystal nucleus that is formed will be "coated" with a layer of gas, in local thermodynamic equilibrium with it. We believe that the initial iridescent phase observed in the bottom of our regime 3 sample is made of such gas-coated crystallites, and that, later on, the upward movement of escaping gas bubbles disturbs the initial gas-liquid interface. When this process has finished, the bottom, iridescent phase appears much compressed because the gas coating of the crystallites has been transferred to the uppermost, bulk gas phase (which therefore increases in size). Note that this kind of behavior is possible *only if* no crystal-liquid common tangent can be drawn on the initial $f(\phi)$ plot ($\mu_p > \mu_p^\dagger$); this confirms that a homogenized three-phase sample indeed has $\mu_p > \mu_p^{\mathrm{tr}}$ (and no common tangent between the three free-energy minima) initially.

In summary, we have discovered experimentally several distinct kinetic regimes within the three-phase triangle of a colloid-polymer mixture. We have shown how the kinetics in each regime, and its approximate location within the triangle, can be predicted by studying the free energy $f(\phi)$. Our work thus exemplifies a generic procedure for obtaining "kinetic maps" from free-energy landscapes. Within our analysis, the form of the free energy places restrictions on the pathways *permitted* within each regime [6]. When more than one possibility remains, the observed pathway will depend on various mobility coefficients and interfacial properties; nonetheless, "educated guesses" (such as those made above for region I) may allow correct prediction without detailed knowledge of these [9]. Mixtures showing multiphase coexistence are widespread in the fundamental study and industrial application of soft condensed matter, e.g., $L_1/L_\alpha/L_3$ coexistence in AOT/oil/brine [10], and isotropic-isotropic-nematic coexistence in mixtures of colloidal rods and nonadsorbing polymer [11]. Thus our procedure should find wide application. Our work also has analogs in simple fluids. The kinetics of phase separation into coexisting vapor, liquid, and solid water in an isolated, constant volume container has been discussed in terms of the energy-volume representation of the phase diagram, in which there is a triangular region of triple coexistence with distinct kinetic regimes [12].

Finally, it is often noted that concavities in the free energy (cf. Fig. 5) are, rigorously, absent: they are "artefacts" of mean-field theories. This is true, but irrelevant; such rigor concerns only the final equilibrium state, *after* phase separation is complete. Mean-field free energies are widely used to predict spinodal decomposition (regime 1) [1]; but their usefulness for other kinetic regimes (regime 2,3) [4] has been largely overlooked. Experiment leaves little doubt that the concavities in $f(\phi)$ have real consequences; the theoretical issue is how, beyond mean-field theory, to define properly the relevant $f(\phi)$ [13].

This work was funded by EPSRC Grant No. GR/K56205. We thank Dr. A. D. Bruce for discussions.

[1] J. D. Gunton, M. San Miguel, and P. S. Sahni, in *Phase Transitions and Critical Phenomena*, edited by C. Domb and J. L. Lebowitz (Academic, London, 1983), Vol. 8, p. 269.
[2] S. M. Ilett, A. Orrock, W. C. K. Poon, and P. N. Pusey, Phys. Rev. E **51**, 1344 (1995).
[3] W. C. K. Poon, Curr. Opin. Colloid Interface Sci. **3**, 593 (1998).
[4] J. W. Cahn, J. Am. Ceram. Soc. **52**, 118 (1969).
[5] H. N. W. Lekkerkerker *et al.*, Europhys. Lett. **20**, 559 (1992).
[6] F. Renth, R. M. L. Evans, and W. C. K. Poon (to be published).
[7] In a monodisperse system, the crystal branch can have two minima [P. Bolhuis and D. Frenkel, Phys. Rev. Lett. **72**, 2211 (1994)].
[8] Recent microscopy observations of Hachisu [Croatica Chem. Acta **71**, 975 (1998)] and Faers and Luckham [Langmuir **13**, 2922 (1997)] of solid forming inside droplets of colloidal liquid can be understood similarly, except that the initial liquid phase in these cases was formed by nucleation and not spinodal decomposition.
[9] M. P. Anisimov *et al.*, J. Chem. Phys. **109**, 1435 (1998).
[10] O. Ghosh and C. A. Miller, J. Phys. Chem. **91**, 4528 (1987).
[11] H. N. W. Lekkerkerker *et al.*, in *Observation, Prediction and Simulation of Phase Transitions in Complex Fluids*, edited by M. Baus, L. F. Rull, and J.-P. Ryckaert (Kluwer, Dordrecht, 1995), p. 53.
[12] P. G. Debenedetti, *Metastable Liquids* (Princeton University, Princeton, NJ, 1996), Chap. 1.
[13] M. E. Fisher and S.-Y. Zinn, J. Phys. A Math. Gen. **31**, L629 (1998); A. D. Bruce (unpublished).